PCCP

Accepted Manuscript

ROYAL SOCIETY OF CHEMISTRY

www.rsc.org/pccp

Rate Constant for the Slow Mu + Propane Abstraction Reaction at 300 K by Diamagnetic RF Resonance

Donald G. Fleming,
TRIUMF Laboratory and Department of Chemistry,
University of British Columbia, Vancouver, BC, Canada, *
and
Stephen P. Cottrell and Iain McKenzie,
ISIS Facility, STFC Rutherford Appleton Laboratory, Didcot, UK,
and
Khashayar Ghandi
Department of Chemistry and Biochemistry,
Mount Allison University, Sackville, NB, Canada.

June 24, 2015

Abstract

The study of kinetic isotope effects for H-atom abstraction rates by incident H-atoms from the homologous series of lower mass alkanes (CH_4, C_2H_6 and, here, C_3H_8) provide important tests of reaction rate theory on polyatomic systems. With a mass of only 0.114 amu, the most sensitive test is provided by the rates of the Mu atom. Abstraction of H by Mu can be highly endoergic, due to the large zero-point energy shift in the MuH bond formed, which also gives rise to high activation energies from similar zero-point energy corrections at the transition state. Rates are then far too slow near 300 K to be measured by conventional TF-μSR techniques that follow the disappearance of the spin-polarised Mu atom with time. Reported here is the first measurement of a slow Mu reaction rate in the gas phase by the technique of diamagnetic Radio Frequency (RF) resonance, where the

*Corresponding Author e-mail:flem@triumf.ca

amplitude of the MuH product formed in the Mu + C_3H_8 reaction is followed with time. The measured rate constant, $k_{Mu} = (6.8 \pm 0.5) \times 10^{-16}$ cm^3 s^{-1} at 300 K, is surprisingly only about a factor of three slower than that for H + C_3H_8, indicating a dominant contribution from quantum tunneling in the Mu reaction, consistent with elementary transition state theory calculations of the k_{Mu}/k_H kinetic isotope effect.

1 Introductory Remarks

The study of kinetic isotope effects (KIEs), the effect of isotopic mass on reaction rates, has a long history, with the most sensitive effects seen from isotopically substituted H atoms: deuterium (D) and particularly here muonium (Mu = μ^+e^-), with a mass of 0.114 amu, the lightest isotope of hydrogen.[1–4] The simplest, and most fundamental chemical reaction is H + H_2, and the isotopic variants of this reaction have played a key role in establishing it as the "benchmark" for comparisons between experiment and reaction rate theory for many years. This has been most recently explored over an unprecedented range of a factor of 36 in H-atom mass in comparing the Mu + H_2 rate with that for the heaviest H-atom, muonic He ($^4He\mu$), with a mass of 4.11 amu,[3,5–8] as well as in comparisons of the rates of Mu and D atoms reacting with vibrationally-pumped H_2,[4–6,9] and in recent papers on "vibrational bonding" at a BrMuBr transition state.[10,11]

Although the only truly accurate potential energy surface (PES) is still for H_3,[3,5,8,12–14] there has also been intense interest in recent years in developing accurate surfaces for the calculation of reaction rates and dynamics for polyatomic systems, notably in the alkanes, [15–27] including isotopic variations by the D and Mu atom reactions with particularly the prototypical H + CH_4 reaction,[16,23,24,26–28] providing important tests of the PESs as well as of the reaction rate theory predicated on them. There are some similarities in the Mu + H_2 [5–8,29,30] and Mu + CH_4[23–28] reactions in that both are highly *endo*ergic reactions due to the huge change in zero-point energy (ZPE) in the MuH product formed, arising from the light Mu-atom mass, giving rise to "late" barriers at the transition state (TS) .[1–3,7,8,16,23,24,30] Though the simplest atom-polyatomic reaction is H + CH_4, comparing isotopic H atom reaction rates with C_2H_6[25,28,31,32] and C_3H_8[25,33,34] are also of interest in this homologous series of lower-mass alkanes, with H + C_3H_8 being of particular interest in comparison with the first results reported herein for the thermal rate constant of the Mu + C_3H_8 reaction in the gas phase.

Previous experimental studies of thermal reaction rates for Mu + CH_4[28] and Mu + C_2H_6[28,31] have been carried out using standard weak transverse magnetic field techniques (TF-μSR). In this technique, the decrease of the initial amplitude of the spin-polarised Mu atom is monitored with time, as a result of MuH formation in the abstraction reaction, where the

muon spin in the diamagnetic product precesses 100-fold slower than in its precursor "triplet" (S = 1) state of muon and electron spins in the Mu atom and is thus dephased with respect to Mu precession in the TF.[1,2,4,8,28,29,31] However, near room temperature (RT) these reaction rates are many orders of magnitude too slow to be measured by this TF-μSR technique. Thus, for example, in the case of the Mu + CH_4 reaction, a rate constant $k_{Mu} \sim 10^{-24}$ cm^3 s^{-1} could be expected at 300 K from extrapolating the results reported in Ref. 28 (and $\sim 10^{-22}$ cm^3 s^{-1} for Mu + C_2H_6 from Ref. 31). Measurements at high temperatures are thus required, in the range $\sim$ 600 K to $\sim$ 900 K for the CH_4 reaction, yielding an activation energy $E_a = 24.6 \pm 0.9$ kcal/mol,[28] the highest yet reported in gas-phase Mu reactivity. Calculations of both the magnitude of the rate constants, $k_{Mu}(T)$, and the measured activation energy for the Mu + CH_4 reaction have met with some success in comparison with both Variational TST calculations[23,24] and reduced dimensionality quantum calculations,[16,26,27] though, with the exception of the work reported in Ref. 26, generally tend to significantly under-predict the experimental rate. This in itself is a statement of the importance of Mu reactivity in assessing the accuracy of reaction rate theory.[5,6]

In contrast to Mu + CH_4, as outlined above, to the best of our knowledge no similarly detailed calculations of the Mu + C_2H_6 reaction rate, in comparison with experiment,[28,31] nor, of particular interest here, Mu + C_3H_8, have been reported. Hot atom reaction yields of Mu with methane and propane are known,[35] but, until the present study, no thermal rates for the Mu + C_3H_8 reaction in the gas phase have been reported. The Mu + C_3H_8 rate was also expected to be too slow near RT for a standard TF-μSR technique to be viable, providing motivation for the present, essentially "proof-of-principle", measurement of the rate constant for this reaction at 300 K by the technique of diamagnetic RF-resonance (RF-μSR), the first measurement of its kind for a *slow* Mu reaction. (The aforementioned Mu + CH_4 and Mu + C_2H_6 reactions, both far too slow to be measured by TF-μSR, are also far too slow near RT to be measured by the present RF technique.) It is hoped that this study will also help to motivate similar theoretical calculations for Mu + C_3H_8 as those reported earlier for Mu + CH_4.[16,23,26,27]

2 Experimental Background and the RF-μSR Technique

2.1 Target environment and μSR signals

The experiments were carried out using the 'EMU' spectrometer located at the 'ISIS' pulsed muon source of the Rutherford Appleton Laboratory (RAL) in the UK.[36] This spectrometer provides a longitudinal magnetic field (LF) up to 5 kG that is ideal for the diamagnetic resonance measurements, but in addition has low transverse field (TF) coils providing fields up to 150 G

perpendicular to the muon spin polarisation.

A beam of 100% spin polarized μ^+ (from π^+ decay), with a kinetic energy of ~ 4 MeV and a lifetime $\tau \sim 2.2$ μs, was implanted in a gas target cell placed in the centre of the spectrometer. The instrument detector arrays, each comprising 48 elements, are located upstream (Forward -'F') and downstream (Backward -'B') relative to the target cell position, which detect the positrons from polarised muon decays ($\mu^+ \rightarrow e^+ \ \nu_e \ \overline{\nu}_\mu$) that are broadcast *preferentially* along the muon spin direction.[2,8,36–38] Decay events from each detector are accumulated over many muon pulses and formed into separate histograms, each of total length 32 μs, with a timing resolution of 16 ns.[36] The anisotropic positron decay pattern results in different count rates being observed in the F/B detectors, defining the average muon "*asymmetry*" (A) of the μSR signal at the time of its decay[2,37,38] (or, equivalently, polarisation, given by the ratio of the measured asymmetry to its maximum value for the conditions of the experiment), defined by

$$A = \frac{N_F - \alpha N_B}{N_F + \alpha N_B} \ , \tag{1}$$

where N_F and N_B are the number of counts in the Forward and Backward detector arrays, respectively, and α is a parameter to correct for different solid-angle counting efficiencies from these detector arrays. Though TFs to ~ 150 G are available on the EMU spectrometer, TF-μSR measurements were run at typically 20 G to provide a measurement of α for each experimental setup, since this essentially gives the maximum amplitude for a Dia signal, given the band pass of the (~ 80 ns) ISIS muon pulse.[36,37]

The target cell was formed by a non-magnetic grade (316) stainless steel (ss) metal cylinder, ~ 20 cm long with an internal diameter of 3.5 cm. The cell is fitted with a front flange holding stacked Ti foils (25 μm each) for a total window thickness of 175 μm, with gas and RF feed-throughs at the other end. The window thickness was adjusted to allow entry of the surface momentum muon beam, while providing sufficient strength to enable working pressures of up to 50 bar. Although the target vessel could be heated above RT, all measurements in the present experiment were carried out at 300 K, monitored by thermocouples attached to the ss body and controlled to better than a degree. It was assumed that the gas, which is in thermal contact with the walls, was at the same temperature, taken then to be 300 ± 1 K.

The RF field was setup by a three-turn saddle coil of length 4 cm and circular cross section of about 5 cm^2, in a fixed position inside the cell, centered about 3 cm from the front window. The RF coil was tuned and matched to 50 Ω at the working frequency of 16 MHz. The resonance condition for diamagnetic muons was determined from a swept field experiment to be 1182 G, and this was used for all RF measurments discussed in this paper. To maintain an optimum RF signal it was important that muon stops were centred within the RF coil. To ensure this, an initial calibration was carried out using pure N_2 gas where the asymmetry (amplitude)

of the RF signal was measured as a function of gas pressure. Optimum pressure was determined by maximum signal, and the value of α was measured for this condition by TF-μSR to provide a check for a similar stopping distribution as other gas mixtures were loaded. The gas target environment was either pure propane at 4.5 bar pressure (limited by the vapour pressure in the cylinder used) or propane/N_2 mixtures, with the propane partial pressure varied to measure the rate constant of interest, k_{Mu}. Both gases were provided from "research grade" commercial gas cylinders. The N_2 partial pressure was adjusted to maintain the same charge density as that of 4.5 bar propane and hence the same muon stopping profile, ensuring consistent RF signals for the different gas mixtures. Earlier experiments with a PEEK cell, an inert polymer, allowed us to place the RF coil outside the cell, so it could easily be positioned to optimise the signal according to the muon stopping distribution.[37,39] However, it transpired that the PEEK outgassed impurities, and therefore this cell design had to be abandoned in favour of the ss vessel used here.

In the present study there are only two muon environments of interest, "diamagnetic" (Dia) and muonium (Mu). The total muon asymmetry is given by $A_{Tot} = A_{Dia} + A_{Mu}$, which is about 0.23 for the conditions of this experiment. The maximum amplitude of the Dia fraction, A_{Dia}, was determined directly from a TF measurement at 20 G, as noted above. A measurement of "triplet" Mu precession in a 2 G TF has an observed signal amplitude $\tilde{A}_{Mu}$, determining the total initial Mu amplitude, $A_{Mu} = 2\tilde{A}_{Mu}$. The factor of two arises from the depolarization of the "singlet" Mu fraction (half) formed during the μ^+ slowing down in the gas.[2,37,39,40] Example TF-μSR signals for the Mu and Dia amplitudes seen in pure propane at a pressure of 4.5 bar are shown in Fig. 1. The amplitude of the Mu signal (Fig. 1 b) contributes directly to the amplitude of the Dia–RF signal from the product MuH formed in the Mu + C_3H_8 reaction, as detailed below.

The measured asymmetries in Fig. 1 are $A_{Dia} = 0.090 \pm 0.003$ and $\tilde{A}_{Mu} = 0.070 \pm 0.02$. The full Mu amplitude, $A_{Mu} = 0.14 \pm 0.04$, accounting for the unobserved singlet fraction, suggests that the fraction of Mu formed, f_{Mu}, is $\sim 60\%$, which is low compared to previous reports of absolute polarizations where this fraction was found to be closer to 70% at a comparable propane pressure.[35] Our TF measurements of the Dia amplitude do not separate contributions due to muon stops in the target walls from the fraction formed in the gas, the latter due to muon molecular ions[37,41] as well as to "hot atom" rections.[35,40] This was determined by separate measurements with 20% O_2 in the target cell, which completely depolarises *all* muons that stop *in* the gas due to repeated electron spin-flip exchange (SE) encounters of Mu with O_2.[42] From this measurement, the muon asymmetry from the walls was found to be ~ 0.03, depending on the stopping environment, and using this adjusted value we obtain excellent agreement for A_{Mu} (and hence f_{Mu}) with earlier results.[35,37]

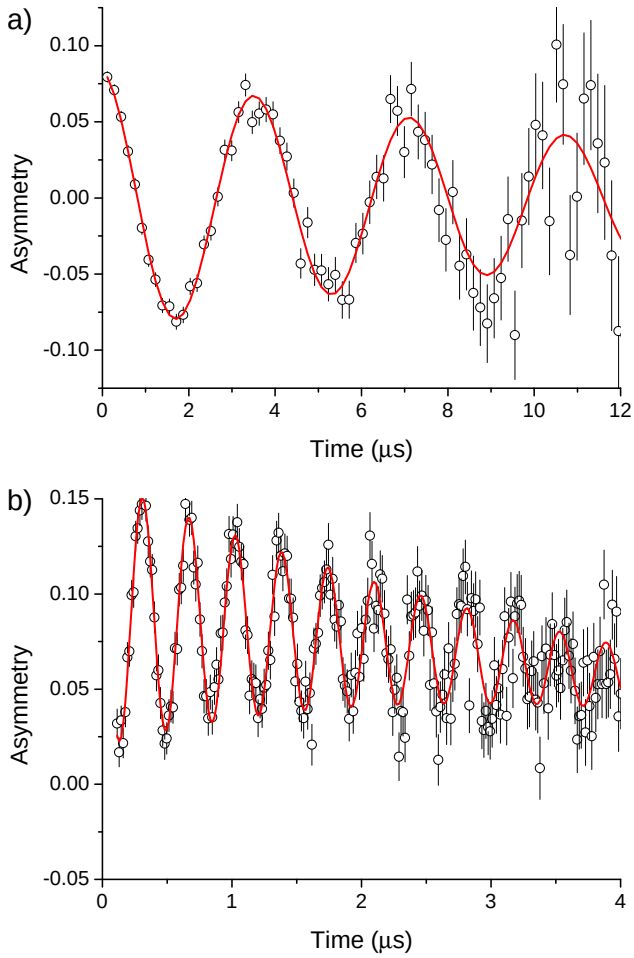

Figure 1: Measured TF-μSR signal amplitudes for muons in diamagnetic environments (Dia, a)), determined from muon precession in a field of 20 G, and for muonium precession (Mu, b)) in a 2 G field, for pure propane gas at 4.5 bar and 300 K. The total initial Dia signal amplitude here is 0.090 ± 0.003 which includes 'wall contributions' of about 0.03. The total Mu amplitude is $A_{Mu} = 0.14 \pm 0.04$, corrected for the loss of 'singlet' Mu. See discussion in the text. The background relaxation rate $\lambda_b = (0.36 \pm 0.03)\ \mu s^{-1}$ that is evident in the fit to the data for Mu precession in b) is mainly due to field inhomogenity ($\Delta B/B \sim 12\%$).

The relaxation of the precessing Mu amplitude evident in Fig. 1 b) is a background effect ($\lambda_b = 0.36 \pm 0.03\ \mu s^{-1}$), mainly due to field inhomogeneity in the TF environment, $\Delta B/B \sim 12\%$, arising from the extended stopping distribution of muons in the gas. Depolarization may also occur through electron SE with gas impurities; oxygen is present at the ppm level in both the propane and nitrogen, making a small contribution to the measured Mu depolarization rate. Only this contribution can be important in the RF experiment, denoted by the parameter 'ν_{SF}', for "spin-flip", in the model developed below. It is noted that the Mu + C_3H_8 chemical reaction rate is far too slow at 300 K to contribute to the relaxation seen in Fig. 1b).

2.2 Kinetics equations

The H-atom abstraction rates from propane by Mu (H,D) proceed via two parallel reaction paths, both giving the same diamagnetic product, MuH; one forming the more stable iso-propyl radical, $CH_3\dot{C}HCH_3$, with a faster expected rate due to abstraction from the central CH_2 moiety,[25] denoted by rate constant k_I; and the other forming the n-propyl radical, $CH_3CH_2\dot{C}H_2$, with rate constant k_N, according to

$$\begin{aligned} \mathrm{Mu} + \mathrm{C_3H_8} &\xrightarrow{k_\mathrm{I}} \mathrm{MuH} + \mathrm{CH_3\dot{C}HCH_3}, \\ \mathrm{Mu} + \mathrm{C_3H_8} &\xrightarrow{k_\mathrm{N}} \mathrm{MuH} + \mathrm{CH_3CH_2\dot{C}H_2}\ . \end{aligned} \tag{2}$$

Since the origin of the MuH product cannot be distinguished by the RF resonance technique employed here (or by a TF-μSR study), we write for the total rate constant $k_{Mu} = k_I + k_N$. Hence the basic kinetics equation for the reactivity of Mu has the form

$$-d[\mathrm{Mu}]/dt = \mathrm{d[Dia]}/dt = k_{\mathrm{Mu}}[\mathrm{Mu}][\mathrm{C_3H_8}] = \lambda_{\mathrm{Mu}}[\mathrm{Mu}] = \lambda_{\mathrm{Mu}}[\mathrm{Mu}]_0\ e^{-\lambda_{\mathrm{Mu}}t}\ , \tag{3}$$

where $[\mathrm{Mu}]_0$ represents the initial "concentration" of Mu atoms. There are only a few hundred muons per beam pulse (~80 ns wide) at ISIS, all of which decay before the next beam pulse (20 ms), but this process is repeated many times, so that Eqn. (3) invokes the "ergodic principle" to describe the reaction rate in terms of the familiar expression for concentrations,[43] where it is the psuedo first-order reaction rate ($[\mathrm{C_3H_8}] >> [\mathrm{Mu}]_0$), λ_{Mu}, that determines the kinetics.[1,28,29,31] From Eqn. (3), the time-dependence of the kinetics 'concentration' of the [MuH] diamagnetic product has the form

$$[\mathrm{MuH}]_\mathrm{t} = [\mathrm{Mu}]_0 \times (1 - \mathrm{e}^{-\lambda_{\mathrm{Mu}}\mathrm{t}})\ , \tag{4}$$

and hence the fractional diamagnetic yield due to Mu reactivity (f_D) has the form

$$f_\mathrm{D} = [\mathrm{MuH}]_\mathrm{t}/[\mathrm{Mu}]_0 = (1 - \mathrm{e}^{-\lambda_{\mathrm{Mu}}\mathrm{t}})\ . \tag{5}$$

Note that as $t \rightarrow 0$ there is no yield, and as $t \rightarrow \infty$ on the scale of the 2.2 μs muon lifetime, all Mu atoms would convert to MuH. However, at long times ($\gtrsim$ 6 μs, see Fig. 1), due to the intrinsic decay of the muon, poor statistics limit the accuracy with which the data can be analyzed in this time domain.

From the calculations reported in Ref. 25 for H-atom reactions with alkanes, in comparison with the data for the Mu + CH_4[28] and Mu + C_2H_6[28,31] reactions, λ_{Mu} is expected to be at least a factor of ten slower for Mu + C_3H_8 compared to H + C_3H_8[25] near RT, giving an anticipated value of $\lambda_{Mu} \lesssim 0.05\ \mu s^{-1}$ at 4.5 bar propane pressure, an order of magnitude less than the background relaxation rate, λ_b, noted earlier (Fig. 1), rendering the measurement of such a slow

rate for the Mu + C_3H_8 reaction by TF-μSR virtually impossible at present conditions. This is the basic motivation for the Dia-RF resonance technique utilized here, where the Mu precursor is held in a stationary state in an applied LF and the amplitude of the Dia MuH product arising from the kinetics scheme of reaction (2) is measured on resonance.[37,44–46]

2.3 The RF-μSR measurements

These studies have been carried out at the ISIS pulsed muon facility at RAL. There is a great advantage in using a pulsed muon beam for RF studies,[37,44,47,48] as opposed to a DC beam,[49,50] in that the RF can be synchronised to the arrival of each muon pulse and need only be applied to the coil for brief periods, ~ 30 μs in these experiments. In contrast, in a DC environment the RF is required to run continuously, causing frequent instabilities due to overheating.

The amplitude of the RF-μSR diamagnetic resonance signal is proportional to f_D of Eqn. (5). In the low TFs of the present study, however, the paramagnetic Mu precursor formed in the 'singlet' state is depolarized and thus would result in a reduced polarization in any final diamagnetic product state formed. RF techniques overcome this loss by effectively decoupling the singlet state while preserving the total phase coherence of the muon polarisation in a high LF, since the implanted muon spin direction is co-linear with the applied field.[37,44–50] Even so, the technique is not a panacea since, if the reaction rate is too slow (as would be the case for both the Mu + CH_4 and Mu + C_2H_6 reactions near 300 K, commented on earlier), there will be insufficient recovery of the final state to measure on the timescale of the μSR experiment. Further complications can arise from using delayed RF measurements[37,48], so the present experiments have all been carried out by zero-delay RF studies based on the technique established by Morozumi et al.[44].

The present study of the Mu + C_3H_8 reaction, with λ_{Mu} expected to be $\lesssim 0.05$ μs^{-1}, as above, is still easily measureable by Dia RF resonance and so then also represents a good 'proof-of-principle' demonstration of the applicability of the RF technique for slow Mu reaction rates. Such a time scale, however, is actually on the border of the lower limit of applicability of the TF-μSR technique, since a value of ~ 0.05 μs^{-1} can be difficult if not impossible to distinquish from background relaxation arising from field inhomogeneity (e.g., λ_b in Fig. 1b)). The RF technique has a huge advantage in this regard, since it is only the muon stops in the gas within the small volume of the RF coil at resonance, in the large applied field, that contribute to the signal.

Following Ref. 44, Eqn. (4) for the simple kinetics concentration of MuH formed from the parallel reactions of scheme (2) at time 't' needs to be modified for an LF–μSR study, rewritten

in terms of the measured Dia amplitude in the *absence* of the RF field[44] as follows:

$$A_{\rm D}(t) = A_{\rm Mu} \times \frac{1+2x^2}{2(1+x^2+\nu_{\rm SF}\tau)} \times (1 - e^{-[1/\tau+\nu_{\rm SF}/(1+x^2)]t}) \ , \qquad (6)$$

where 'x'= B/B_{Hf}, with B the applied LF and $B_{Hf} = \nu_0/\gamma_e = 1593$ G is the contact hyperfine field of the μ^+ at the electron in the Mu atom, where $\nu_0 = 4463.3$ MHz is the vacuum Mu hyperfine coupling constant and $\gamma_e = 2.8025$ MHz/G; $\lambda_{\rm Mu} = 1/\tau$, the psuedo first-order relaxation rate with τ the mean lifetime for chemical reaction from the reaction scheme in Eqn. (2) and $\nu_{\rm SF}$ is the SF rate introduced above. Though this is often due to the interaction of the Mu atom with different paramagnetic centers in solid-state environments,[44] in the gas phase it can realistically only be due to SE from small amounts of O_2 impurity in either the reactant propane or nitrogen moderator, manifest as a contribution to the relaxation of the T_2 signal shown in Fig. 1 b). The amplitude $A_{\rm Mu}$ is the total Mu amplitude (twice the observed value, $\tilde{A}_{\rm Mu}$), with muonium formed promptly during the slowing-down processes of the μ^+,[39,40] also exemplified by the data in Fig. 1 b) for pure propane at 4.5 bar, where $A_{\rm Mu} = 0.14 \pm 0.04$.

In addition, there is a "prompt" diamagnetic signal formed at early times, during the final slowing-down processes of the muon in the gas at kinetic enegies $\lesssim 10$ eV,[2,35,39,40] due either to the formation of muon molecular ions[37,41] or to MuH (as in Eqn. 2), or both, formed from epithermal (hot) Mu reactions. For the latter case, it is likely that the n-propyl radical product is more strongly formed at epithermal energies, well above k_BT, than at thermal energies.[25] Since this happens *during* the slowing-down time it is reflected in the initial Dia amplitude, and contributes to the signal seen in Fig. 1 a). This signal also includes muon stops in the walls (~ 0.03, as in Fig. 1 above); however, these stops do not contribute to the RF signal as they are outside the RF field. The 'prompt' Dia MuH fraction formed in the gas and within the RF coil is denoted here by A_P. Although it would seem reasonable to assume that this fraction would be the same as that determined previously in pure propane,[35] approximately 0.05 for the 4.5 bar conditions of the present experiment, it is not known for the propane/N_2 mixtures of interest in the RF experiment, where $N_2\mu^+$ molecular ions may also be formed.[37,41] There may also be some variation between measurements due to beam instabilities. Consequently, the time-independent prompt value, A_P, for MuH formation, is treated as a fitted free parameter for each measurement in the analysis that follows. See descriptions of these parameters in Table I.

Table I: Description of the parameters that enter Eqn. (8) in fiting the RF data for Mu + C_3H_8.

Parameter	Description
A_P	The prompt diamagnetic amplitude.
A_D	The diamagnetic amplitude formed by reaction.
$A_{T,Dia}$	The initial diamagnetic amplitude at 20 G, contributions from A_P and A_D.
A_{Mu}	The initial total Mu amplitude. Determined from 2 G TF measurements.
B	The Longitudinal Field on Resonance, 1182 G.
ν_1	The diamagnetic precession frequency on resonance, determined by calibration.
λ_1	The relaxation rate due to B_1 inhomogeneity, also calibrated.
ν_0	The hyperfine coupling constant for the vacuum Mu atom, 4463.3 MHz.
ν_{SF}	The spin flip rate, estimated from T_1 relaxation at the applied field on resonance.
τ	The mean conversion time for the Mu + C_3H_8 reaction, $\tau = 1/\lambda_{Mu}$.

On resonance, a transition betweeen two muon magnetic sub-states is observed in a time differential measurement of the F-B asymmetry of decay e^+ events, which exhibits a spin precession around the applied RF field, B_1.[37,44–50] The observed *total Dia* asymmetry, $A_{T,Dia}(t)$, is then a sum of the prompt fraction, A_P, and that of the diamagnetic species formed by the later reaction of Mu in the *presence* of the RF field, the second term in Eqn. (7), giving at observation times

$$A_{T,Dia}(t) = A_P \times e^{-\lambda_1 t} cos(2\pi\nu_1 t) + \int_0^t (dA_D/dt') e^{-\lambda_1 (t-t')} \times cos 2\pi\nu_1 (t-t')\, dt' \ , \qquad (7)$$

where $(dA_D/dt') = \lambda_{Mu}[Mu]_0\ e^{-\lambda_{Mu} t'}$ from Eqn. (3) and $\nu_1 = \gamma_\mu B_1$, with γ_μ the muon gyromagnetic ratio = 0.01355 MHz/G, and λ_1 is a relaxation of the resonance signal due to the field inhomgeneity of the RF coil.

Since both ν_1 and λ_1 are highly correlated, it is important to calibrate them against measurements of the RF signal in a non-reactive environment, at constant charge density in the gas, where the Dia fraction should then be constant in time. As mentioned earlier, an initial calibration was made from on-resonance measurements of the Dia amplitude in pure N_2 at 8.5 bar, an equivalent density to that of the maximum propane pressure of 4.5 bar. It was found, however, that there were clear differences in fitted values for these parameters when propane was introduced into the cell, perhaps arising from differences in the dielectric constants for these gases, causing a change in the 'Q' of the tuned circuit. So an additional calibration was made for 0.8 bar propane partial pressure in N_2 at a total pressure of 7.7 bar (same density); at this low propane partial pressure the conversion rate due to reaction with propane (second term of

Eqn. 7) is slow enough so as to not appreciably change the Dia amplitude from muon stops within the RF coil, allowing a recalibration of the values of ν_1 and λ_1.

Assuming the same time-independent background effects for the F and B detectors and neglecting higher order terms that might contribute to Eqn. (7), an effective resonance signal, S_{RF}, due to the formation of the Dia MuH product on resonance, can be defined from Eqn. (1) by

$$S_{\mathrm{RF}}(t) = \left[\frac{N_F - \alpha N_B}{N_F + \alpha N_B}\right]^{\mathrm{ON}} - \left[\frac{N_F - \alpha N_B}{N_F + \alpha N_B}\right]^{\mathrm{OFF}} = A_{\mathrm{T,Dia}}(t) - [A_{\mathrm{P}} + A_{\mathrm{D}}(t)] \ , \qquad (8)$$

where 'ON' and 'OFF' correspond to the measured muon asymmetries for the RF-on and RF-off, respectively, with data acquisition interleaved between the two states, alternately taking 500 pulses with RF-on and 500 with RF-off. This method of data acquisition is designed to reduce the effects of equipment instability and to uniquely reveal the response of muons in diamagnetic environments in the gas at resonance, with background signals removed. The prompt fraction, A_P, is defined above and $A_D(t)$ is given by Eqn. (6).

3 Simulations and Experimental Results

Although the equations discussed above require several parameters to describe the RF signal, $S_{RF}(t)$ of Eqn. (8), some are known and/or can be fixed from TF and RF calibration measurements. Those that are known are the on-resonance field, 1182 G (LF), which corresponds to the field required for resonance of the Dia species with an RF coil tuned to a frequency of exactly 16 MHz, and the Mu hyperfine coupling constant, $\nu_0 = 4463.3$ MHz in vacuum.[2,38] One parameter can be determined and one estimated from off-resonance TF measurements: the total initial Mu amplitude for muon stops in pure propane A_{Mu}, determined from the results seen in Fig. 1b), as explained earlier; and the prompt diamagnetic amplitude, A_P, in the propane, determined in the absence of RF from a TF run at 20 G, exemplified by the data in Fig. 1a), respectively. As previously commented, the latter has to be corrected for muon stops in the ss walls of the target vessel, determined by adding about 20% O_2 to the target gas, which completely depolarizes all muons that stop in the gas.[2,39] Nevertheless, this corrected value only serves as a good inital guess due to the aforementioned uncertainties in determining A_P for the propane/N_2 gas mixtures used, so that this parameter was also determined by treating it as a fitting parameter in the analysis that follows.

There are four other parameters that need to be considered when fitting these RF measurements: the precession frequency about the B_1 (RF) field, ν_1; the relaxation rate due to the inhomogeneity of this field, λ_1; the spin flip rate of the Mu atom, ν_{SF}; and particularly

the chemical reaction rate of interest, $\lambda_{Mu} = 1/\tau$, where τ is the conversion time from Mu to diamagnetic MuH due to reaction (2). The fitted results can be strongly dependent on values chosen for these parameters, which are highly correlated. Fortunately, with the exception of the conversion time, τ, which is the subject of the experiment, it is possible to obtain a good estimate for each parameter from calibration measurements, enabling them to be fixed during fitting of the RF data.

Both ν_1 and λ_1 can be found from time-differential (TD) measurements of the RF precession frequency in the absence of state conversion, at constant gas density, either in pure N_2 or at a low partial pressure of propane (0.8 bar), with values recorded in Table II below for the latter case. The Mu atom SF rate ν_{SF} can be found from TD spin relaxation (T_1) measurements of the gas mixture being measured at the static applied field (1182 G), also recorded in Table II. (The errors on these fitted values were typically ± 5%.) In high longitudinal fields the only viable mechanism for T_1 spin relaxation is Mu atom spin exchange with impurity O_2 in the gas sample, which is well known to be quenched in a LF field by a factor $1/(1 + x^2)$,[2,38,51] where 'x' has been defined above. Since the Mu hyperfine field (B_{Hf} = 1593 G) is close to the same value as the applied field of 1182 G, corresponding to the RF resonance frequency of 16 MHz, 'x' ∼ 1, and therefore at low fields, from the average of the entries in Table II, ν_{SF} would be ∼ 0.06 μs^{-1}. This would correspond to an impurity level of ∼ 1.5 ppm in the gas sample, entirely consistent with expected impurity levels in the gases used. It is noted that this value of ∼ 0.06 μs^{-1} for the Mu relaxation rate at low fields, due to SE with impurity O_2 in the sample, is small compared to the measured value of 0.36 μs^{-1} by TF-μSR seen in Fig. 1, consistent with the previously stated view that the latter is mainly due to field-inhomogeneity arising from the extended muon stopping distribution in the gas.

Simulations were carried out to investigate the form of the RF signals, $S_{RF}(t)$, as a function of reaction time, τ, for the zero delay RF experiment, as shown in Fig. 2. Fixed parameters were chosen to represent conditions in the current experiment, from the calibrations carried out at a propane partial pressure of 0.8 bar (Table II below): $A_P = 0.0157$, $A_{Mu} = 0.169$, B = 1182 G, $\nu_0 = 4463$ MHz and $\nu_{SF} = 0.012$ μs^{-1}, with values for ν_1 and λ_1 taken as described above, 0.116 MHz and 0.272 μs^{-1}, respectively.

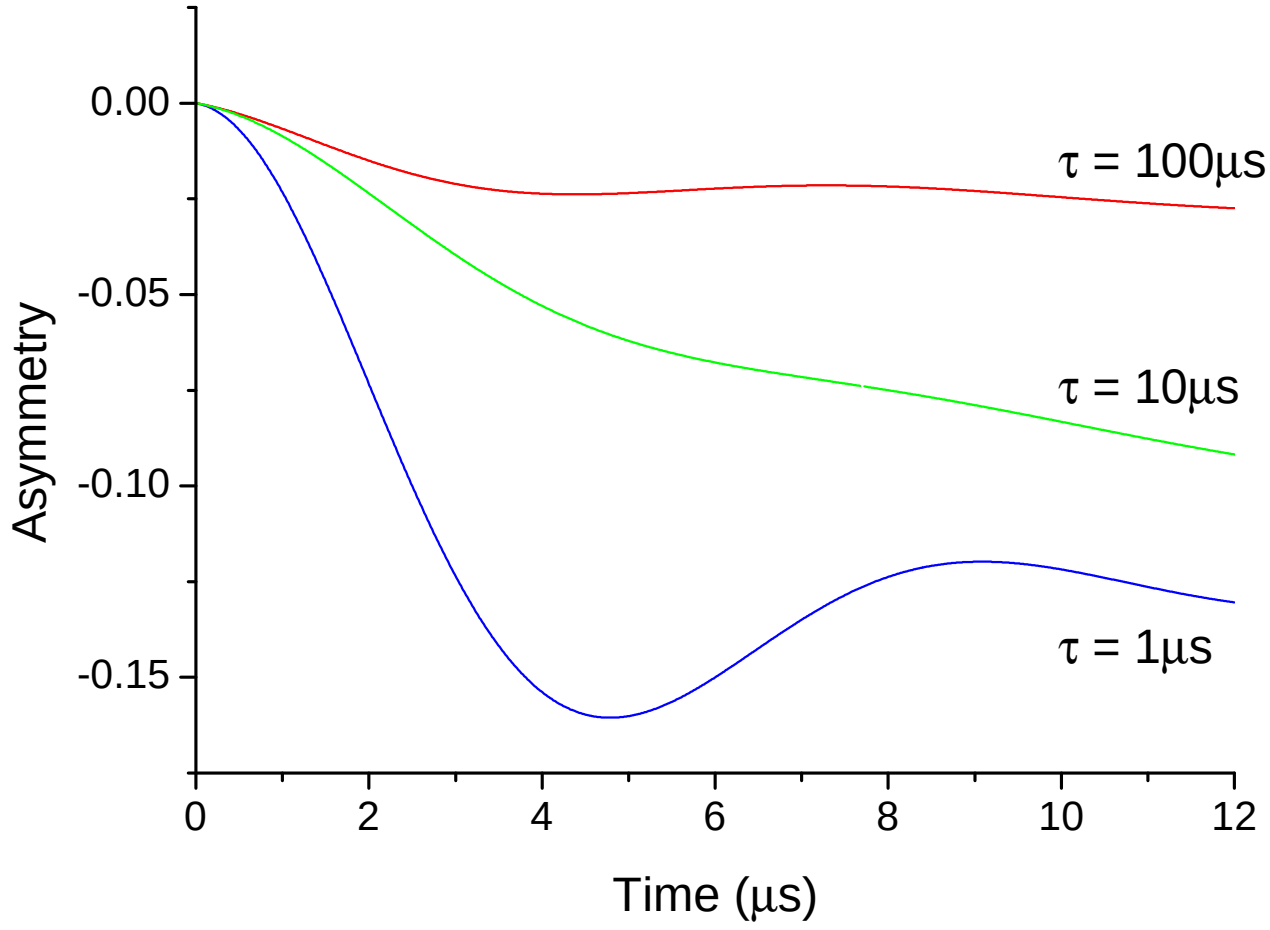

Figure 2: Simulations investigating the form of $S_{RF}(t)$ as a function of reaction time τ ($= 1/\lambda_{Mu}$). Modelling based on Eqn. (8) describing RF Dia resonance measurements for the slow H-atom abstraction rates assumed for the Mu + C_3H_8 reaction. Simulations are shown for different values of τ: 100 μs (red curve), 10 μs (green curve) and 1 μs (blue curve). (The latter would actually correspond to a much higher propane pressure than allowed by the experimental conditions.) All other parameters are fixed at values as discussed in the text.

Representative data from the present experiment for the Mu + C_3H_8 reaction at selected propane partial pressures, together with fits to Eqn. (8), are shown in Fig 3. Curves are shown for the lowest propane partial pressure of 0.8 bar in N_2 (top), for a propane partial pressure of 3.0 bar in N_2, (middle) and for pure propane at 4.5 bar (bottom), all at the same total charge density corresponding to 8.4 bar N_2 at 300 K. These data reflect the general trends seen in the simulations shown in Fig. 2; in particular, the two lower plots in Fig 3 have lifetimes τ within a factor of two of the 10 μs result shown in Figure 2 (green curve) while the upper plot is close to that of the upper simulation for $\tau = 100$ μs. The results of these fits, together with those obtained at intermediate propane partial pressures, are given in Table II.

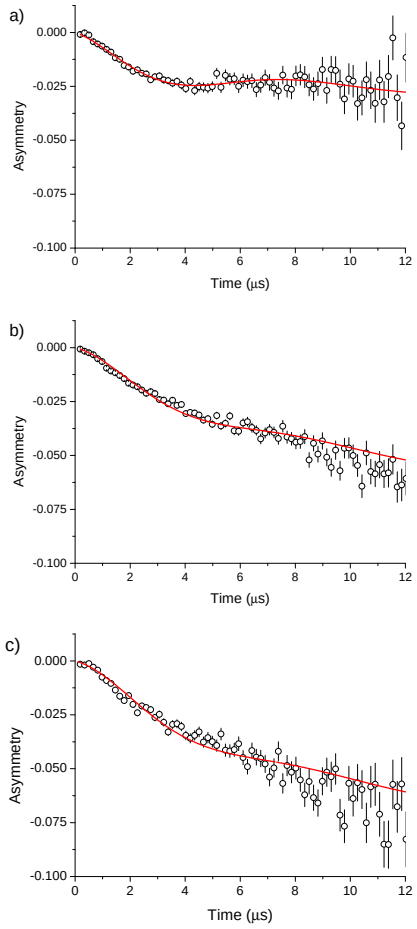

Figure 3: Results for the measured Dia-RF data for the Mu + C_3H_8 reaction at selected propane partial pressures: (top) for a propane partial pressure of 0.8 bar in N_2, (middle) for a partial pressure of 3.0 bar in N_2 and (bottom) for pure propane at 4.5 bar pressure, all at the same total charge density corresponding to 8.4 bar of pure N_2. The solid lines shown are fits of Eqn. (8) to the RF data. These data reflect the general trends seen in the simulations shown in Fig. 2.

The central results of these experiments are the values of the relaxation rates $\lambda_{Mu} = 1/\tau$, the last two columns of Table II, where τ is determined from fits to the data as shown in Fig. 3. Note that these values for λ_{Mu} are also all much less than the background relaxation rate λ_b seen from the TF-μSR data in Fig. 1. They are plotted as a function of propane partial pressure in Fig. 4 (solid blue triangles) and fit to the expected straight line dependence (blue line)

$$\lambda_{Mu} = \lambda_0 + k_{Mu}[C_3H_8] \ , \tag{9}$$

where λ_0 is a background relaxation in the absence of propane ($\neq \lambda_b$) and k_{Mu} is the bimolecular rate constant of interest. Eqn. (9) reflects the psuedo first-order nature of the kinetics outlined earlier. The slope of the fitted blue line shown gives $k_{Mu} = (6.67 \pm 0.38) \times 10^{-16}$ cm^3 s^{-1}, with a background intercept (λ_0) that is zero.

Table II: Results of global fits determining λ_{Mu} from parameter variations of Eqn. (8) for the Mu + C_3H_8 reaction at 300 K. RF parameters (columns 4 and 5) determined by calibration at 0.8 bar propane partial pressure. See earlier discussion in the text. Values previously determined and fixed during the fitting of Eqn. (8) to the data are shown without error. The rates λ_1, ν_{SF} and λ_{Mu} are all in units of μs^{-1}.

C_3H_8 in bar	A_P	A_{Mu}	ν_1 (MHz)	λ_1	ν_{SF}	λ_{Mu}	τ (μs)
4.5	0.0121(1)	0.140	0.116	0.272	0.028	0.069(2)	14.5
3.8	0.0112(1)	0.143	0.116	0.272	0.022	0.065(3)	15.4
3.0	0.0117(1)	0.149	0.116	0.272	0.031	0.050(1)	20.0
2.0	0.0192(1)	0.150	0.116	0.272	0.026	0.031(1)	32.2
1.2	0.0177(1)	0.153	0.116	0.272	0.043	0.021(1)	47.6
0.8	0.0157(1)	0.169	0.116	0.272	0.012	0.009(2)	111

As previously commented, an absolute calibration of the RF parameters, ν_1 and λ_1, in these propane mixtures was difficult to achieve, perhaps due to changing dielectric constants in the gas, so it was important to investigate how an uncertainty in these parameters might affect the fitted value for k_{Mu}. From an initial calibration carried out for muons stopped in pure N_2 gas at 8.5 bar, the same total charge density as 4.5 bar propane, slightly different values for the RF parameters were obtained, $\nu_1 = 0.085$ MHz and $\lambda_1 = 0.3$ μs^{-1}, compared to the entries in Table II. The fitting of the reaction rate data with propane was then repeated with the identical procedure but substituting these modifed RF parameters as fixed values, giving the

results shown by the solid red circles in Fig. 4. In this case the best fit (red) straight line gives $k_{Mu} = (7.06 \pm 0.47) \times 10^{-16}$ cm^3 s^{-1}, but here with a background intercept of -0.0111 $\pm$ 0.0024 μs^{-1}. The unphysically negative value of this intercept reflects the aforementioned difficulty of determining the RF parameters. However, it is important to note that this makes little or no difference to the slope of the fitted line.

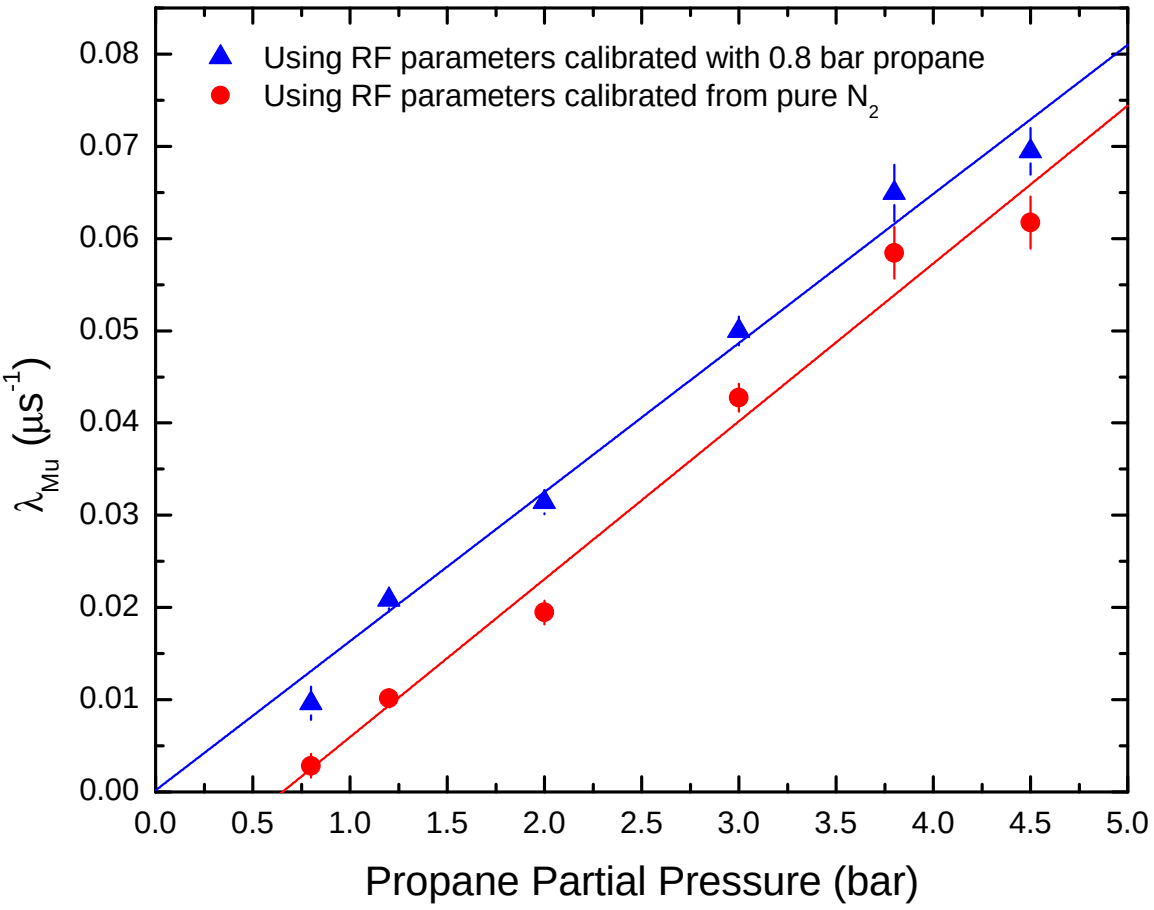

Figure 4: Plot of the fitted results for λ_{Mu} from Table II at 300 K as a function of the C_3H_8 partial pressure, shown by the solid-blue triangles. The RF parameters were determined by calibration at 0.8 bar propane. The blue line is a fit of Eqn. (9) to the data, giving the rate constant $k_{Mu} = (6.7 \pm 0.4) \times 10^{-16}$cm^{3}s^{-1} The solid red circles and fitted red line have been determined from a similar fitting procedure, but now using RF paramaters $\nu_1 = 0.085$ MHz and $\lambda_1 = 0.3$ μs^{-1}, derived from a calibration done in pure N_2 (see text), giving $k_{Mu} = (7.1 \pm 0.5) \times 10^{-16}$cm^{3}s^{-1}. The results are the same, within error. More accurate values of k_{Mu} are given in the text.

A weighted average of the two fitted results from this analysis gives $k_{Mu} = (6.82 \pm 0.29) \times 10^{-16}$ cm^3 s^{-1}. However, in view of the discussion above that some systematic error could be introduced as a result of small changes in the RF parameters arising from the two different calibrations carried out, we feel it is prudent to broaden the overall error on the fitted result from Fig. 4, giving a final reported result for $\langle k_{Mu} \rangle = (6.8 \pm 0.5) \times 10^{-16}$cm^3 s^{-1} for the Mu + C_3H_8 reaction at 300 K. It is this value upon which the discussion that follows is based.

4 Discussion and Concluding Remarks

The measured (averaged) thermal rate constant for the slow Mu + C_3H_8 reaction by the present Dia-RF resonance study, $\langle k_{Mu} \rangle = (6.8 \pm 0.5) \times 10^{-16}$ cm^3 s^{-1} at 300 K, could not accurately be determined at this temperature by the standard TF-μSR technique.[28,31] This would require propane partial pressures of $\sim$ 60 bar to give an easily measurable relaxation rate of $\lambda_{Mu} \sim 1$ μs^{-1}. At such densities, other contributions to measured relaxation rates from radiation-induced "spur effects" begin to play a role,[35,52] which can then render the interpretation of any relaxation rate data in terms of basic kinetics as suspect. The present measurement is therefore much better suited to study by Dia-RF resonance and, as such, being the first measurement of its kind for a *slow* H-atom abstraction reaction, can also be thought of as a 'proof-of-principle' confirmation of the technique.

As previously remarked, there appears to have been no theoretical calculations reported for the Mu + C_3H_8 reaction, the only such calculations in alkanes having been for the Mu + CH_4 reaction.[16,23,24,26,27] From the results given in Ref. 25, the rate constant for H + C_3H_8 at 300 K, $k_H \sim 2 \times 10^{-15}$ cm^3 s^{-1} (estimated from Fig. 5 in that paper), appears to agree well with experiment,[33,34] but, suprisingly, is only about three times faster than that for the much more endoergic Mu + C_3H_8 reaction found here, a KIE $k_{Mu}/k_H \sim 1/3$, from the values above. From basic transition state theory (TST), we could expect the H-atom rate to be favoured over the Mu reaction by a factor of *1000*, as outlined below.

The classic expression for the rate constant for an A + BC reaction in TST[53] has the form

$$k(T) = \Gamma(T) \frac{k_B T}{h} \frac{Q^{\ddagger}_{TS}}{Q_A Q_{BC}} e^{-(E^{\ddagger}_0/k_B T)} \qquad (10)$$

where the Q are Partition Functions (PFs), $\Gamma(T)$ is an ad-hoc correction due to quantum tunneling in what is otherwise a classical formalism, and $E^{\ddagger}_0$ at the TS has the form

$$E_0^{\ddagger} = V_S^{\ddagger} + \sum_j E_{j,0}^{\ddagger} - \sum_i E_{i,0}(RH) \ , \tag{11}$$

where $V_S^{\ddagger}$ is the electronic barrier height at the saddle point, $E_{j,0}^{\ddagger}$ represents the zero-point energy (ZPE) of the j'th vibrational level at the TS and $E_{i,0}$ are these values for the RH reactant.

For most *exo*ergic or "early-barrier" reactions, the TS tends to more closely resemble the reactants and the barrier height at the saddle point is at or near the maximum of the minimum energy path (MEP), which has a relatively weak dependence then on isotopic mass.[30] However in the case of *endo*ergic or "late barrier" reactions, which is the case here for Mu + C_3H_8, the saddle point is shifted toward the product valley and the TS more closely resembles the MuH product.[5,6,23,30] The H-abstraction reactions from a C−H bond in alkanes by incident H-atoms are nearly thermoneutral or slightly endoergic for methane ($\sim$ 0.6 kcal/mol), becoming exoergic (-3.1 kcal/mol) for the H + C_3H_8 reaction,[25] but are uniformly endoergic for the isotopic analog Mu reactions, from $\sim$ +7.5 kcal/mol for CH_4[23,26] to about +4.3 kcal/mol expected for propane, due to the huge ZPE shift in the MuH product formed that arises from the light Mu-atom mass.[23,30] This also has the effect of giving large ZPE contributions to the values of $E_{j,0}^{\ddagger}$ at the [Mu-H$\cdots$ C_3H_7]‡ TS in Eqn.(11).

Thus, in comparing the reaction rates for H + C_3H_8 and Mu + C_3H_8, from Eqn. (10), we can write for the KIE (same reactant),

$$k_{\rm Mu}/k_{\rm H} = \Gamma_{\rm Mu}/\Gamma_{\rm H} \times Q_{\rm trans,H}/Q_{\rm trans,Mu} \times Q^{\ddagger}_{\rm rot,Mu}/Q^{\ddagger}_{\rm rot,H} \times e^{\Delta V_{\rm S}^{\ddagger}/k_BT} \times e^{-[(\sum_j E^{\ddagger}_{\rm j,0,Mu}/k_BT - \sum_j E^{\ddagger}_{\rm j,0,H}/k_BT]} \tag{12}$$

where the ratio of translational and vibrational PFs at the TS is near unity and $\Delta V_{\rm S}^{\ddagger} = V^{\ddagger}_{\rm S,H}$ - $V^{\ddagger}_{\rm S,Mu}$ is the difference in saddle point potential maxima, and can only be properly determined from Variational TST.[3,5,6,8,23,30,54]

To estimate a value for this KIE in the *absence* of tunneling ($\Gamma_{\rm i} = 1.0$), we assume that the frequencies at the variational position of the TS ([H-H$\cdots$$C_3H_7$]‡) are largely determined by the ZPE of the single stretch of the H–H or Mu–H product, or about 2200 cm^{-1} and 4800 cm^{-1}, respectively; scaling, as a first approximation, by the reduced mass of the diatomic product isotopomer. Though admitedly an overly simplified assumption, it can be noted that a similar difference is found in Ref. 23 (Table XIV) in comparing TST results for H + CH_4 and Mu + CH_4, in which the ZPE changes from a normal mode analysis at the TS were accounted for. The present approximation gives for the 2nd exponent in Eqn. (12) a factor of $\sim 4 \times 10^{-6}$ at 300 K. The first exponent, due to the difference in barrier heights arising from different saddle point positions can be expected to favour the Mu reaction by a factor of $\sim$10 .[5,6,30] The ratio of translational PFs ($\propto \mu^{3/2}$) for the reduced mass of the H atom in the entrance channel is a

factor of 25 in favour of Mu, with the ratio of rotational PFs at the TS ~ 0.5 depending on its variational location. These combined factors from Eqn. (12) give $k_{Mu}/k_H \sim 0.5 \times 10^{-3}$ at 300 K.

Although this result is just a crude estimate based on simple TST and a simplified assumption of ZPEs at the TS (lacking a normal mode analysis), nevertheless, in comparison with the ratio mentioned above of $k_{Mu}/k_H \sim 1/3$ from experiment and the quantum calculations of Kerkeni and Clary for H + C_3H_8,[25] it does suggest a large contribution from quantum tunneling to the Mu + C_3H_8 reaction near 300 K ($\Gamma_{Mu} \gg 1$). However, this can only be reliably determined from a full quantum calculation of the reaction rate since the estimates of Γ_{Mu} for quantum tunneling in VTST can depend quite crucially on the nature of the tunneling path chosen and particularly its width.[6,8,22–24,30] From the 2D quantum calculations of Ref. 25, the tunneling enhancement due to H is about a factor of 10 in comparison with their classical TST calculation. It could well be two orders of magnitude greater for the Mu reaction rate, which would then bring the simple TST estimate of k_{Mu}/k_H above to about 0.1, much closer to experiment. The importance of quantum tunneling in the Mu + C_3H_8 reaction rate can also be assessed by a planned measurement of the activation energy for this reaction. If Mu tunneling in this reaction is indeed as large as the present TST estimate suggests, a very weak temperature dependence should be seen.

5 Acknowledgements

We are grateful to support provided by the European Commission under the 7th Framework Programme through the Key Action: Strengthening the European Research Area, Research Infrastructures; Contract No: CP-CSA_INFRA-2008-1.1.1 Number 226507-NMI3, for the development of the gas sample pressure cells with integral RF coils, together with support for visits by DGF to develop the scientific programme. DGF also thanks the Centre for Molecular Structure and Dynamics and the Science and Technology Facilities Council in the UK for supporting part of this work and as well NSERC (Canada) for their continuing grant support.

References

[1] S. Baer, D. Fleming, D. Areseneau, M. Senba and A. Gonzalez, in *Isotope Effects in Chemical Reactions and Photodissociation Processes*, ACS Symposium Series 502, Washington, DC, 1992, pg. 111.

[2] D.G. Fleming and M. Senba, in *Progress in Meson Science*, Kodansha Press, Tokyo, 1992.

[3] D.G. Fleming, D.J. Arseneau, O. Sukhorukov, J.H. Brewer, S.L. Mielke, G.C. Schatz, B.C. Garrett, K. A. Peterson and D.G. Truhlar, *Science*, 2011, **331**, 448.

[4] P.Bakule, D.G. Fleming, O. Sukhorukov, K.Ishida, F.Pratt, T. Momose, E. Torikai, S.L. Mielke, B.C. Garrett, K.A. Peterson, G.C. Schatz and D.G. Truhlar, *J. Phys. Chem. Lett.*, 2012, **3**, 2755.

[5] S.L. Mielke, B.C. Garrett, D.G. Fleming and D.G. Truhlar, *Mol. Phys.*, 2015, **113**, 160.

[6] J. Aldegunde, P.G. Jambrina, E. Garci′a, V.J. Herreo, V. Sa′ez-Ra′banos and F.J. Aoiz, *Mol. Phys.*, 2013, **111**, 3169.

[7] P.G. Jambrina, E. Garcia, V.J. Herrero, V. S.-Ra′banos and F.J. Aoiz, *J. Chem. Phys.*, 2011, **135**, 034310.

[8] D.G. Fleming, D.J. Arseneau, O. Sukhorukov, J.H. Brewer, S.L. Mielke, D.G. Truhlar, G.C. Schatz, B.C. Garrett and K.A. Peterson, *J. Chem. Phys.*, 2011, **135**, 184310. 2011.

[9] P.G. Jambrina, E. Garcia, V.J. Herrero, V. S.-Ra′banos and F.J. Aoiz, *Phys. Chem. Chem. Phys.*, 2012, **14**, 14596.

[10] D.G. Fleming, S.P.Cottrell, I.McKenzie and R.M. Macrae,*Phys. Chem. Chem. Phys.*, 2012, **14**,10953.

[11] D.G. Fleming, J. Manz, K. Sato and T. Takayanagi, *Angew. Chem. Int. Ed.*, 2014, **53**, 13706.

[12] S. L. Mielke, K.A. Peterson, D.W. Schwenke, B.C. Garrett, D.G. Truhlar, J.V. Michael, M-C. Su and J. W. Sutherland, *Phys. Rev. Lett.*, 2003, **91**, 063201.

[13] S.L. Mielke, D.W. Schwenke and K.A. Peterson, *J. Chem. Phys.*, 2005, **122**, 224313.

[14] S.L. Mielke, D.W. Schwenke, G.C. Schatz, B.C. Garrett and K.A. Peterson, *J. Phys. Chem. A*, 2009, **113**, 4479.

[15] J.P. Cambden, H.J. Bechtel, D.J.A. Brown, M.R. Martin, R.N. Zare, W. Hu, G. Lendvay, D. Troya and G.C. Schatz, *J. Am. Chem. Soc.*, 2005, **127**, 11898.

[16] Y. Li, Y.V. Suleimanov, J.Li, W.H. Green and H. Guo, J. Chem. Phys., 2013, **138**, 094307.

[17] S. Liu, J. Chen, Z. Zhang and D.H. Zhang, J. Chem. Phys., 2012, **138**, 011101.

[18] R. Liu, H. Xiong and M. Yang, J. Chem. Phys., 2012, **137**, 174113.

[19] Y. Zhou, B. Fu, C. Wang, M.A. Collins and D.H. Zhang, J. Chem. Phys., 2011, **134**, 064323.

[20] T. B. Alby, J. Espinosa-Garcia and D.G. Truhlar, Chem. Rev., 2007, **107**, 5101.

[21] Z. Xie, J.M. Bowman and X. Zhang, *J. Chem. Phys.*, 2006, **125**, 133120.

[22] J. Pu and D.G. Truhlar, J. Chem. Phys., 2002, **116**, 1468.

[23] J. Pu and D.G. Truhlar, J. Chem. Phys., 2002, **117**, 10675.

[24] J. Espinosa-Garcia, *Phys. Chem. Chem. Phys.*, 2008, **10**, 1277.

[25] B. Kerkeni and D.C. Clary, *Phys. Chem. Chem. Phys.*, 2006, **8**, 917.

[26] B. Kerkeni and D.C. Clary, Chem. Phys. Letts., 2006, **421**, 499.

[27] S.T. Banks, C.S. Tautermann, S.M. Remmert and D.C. Clary, J. Chem. Phys., 2009, **131**, 044111.

[28] R. Snooks, D.J. Arseneau, D.G. Fleming, M. Senba, J.J. Pan, M. Y. Shelley and S. Baer, J. Chem. Phys., 1995, **102**, 4860.

[29] I.D. Reid, D.M. Garner, L.Y. Lee, M. Senba, D.J. Arseneau and D.G. Fleming, *J. Chem. Phys.*, 1987, **86**, 5578.

[30] B.C. Garrett, R. Steckler and D.G. Truhlar, *Hyp. Int.*, 1986 **32**, 779.

[31] R. Snooks, D.J. Arseneau, S. Baer, D.G. Fleming, M. Senba, and M. Y. Shelley, *Hyp. Int.*, 1994, **87**, 911.

[32] M.G. Bryukov, I.R. Slagle and V.D. Knyazev, *J. Phys. Chem. A*, 2001, **105**, 6900.

[33] R.M. Marshall, H. Purnell and A. Sheppard, *J. Chem. Soc. Far. Trans. I*, 1984, **80**, 2999.

[34] W. Tsang, *J. Phys. Chem. Ref. Data*, 1988, **17**, 887.

[35] J.R. Kempton, D.J. Arseneau, D.G. Fleming, M. Senba, A.C. Gonzalez, J.J. Pan, A. Tempelmann and D.M. Garner, *J. Phys. Chem.*, 1991, **95**, 7338.

[36] S.R. Giblin, S.P. Cottrell, P.J.C. King, S. Tomlinson, S.J.S. Jago, L.J. Randall, M.J. Roberts, J. Norris, S. Howarth, Q.B. Mutamba, N.J. Rhodes and F.A. Akeroyd, *Nucl. Inst. and Meth.*, 2014, **A 751**, 70.

[37] C. Johnson, S.P. Cottrell, K. Ghandi and D.G. Fleming, *J. Phys. B*, 2005 **38**, 119.

[38] E. Roduner, *Appl. Mag. Res.*, 1997, **13**, 1.

[39] M. Senba, D.J. Arseneau, J.J. Pan and D.G. Fleming, *Phys. Rev. A.*, 2006, **74**, 042708.

[40] M. Senba, D.G. Fleming, D.J. Arseneau and H. Mayne, *J. Chem. Phys.*, 2000, **112**, 9390.

[41] D.J. Arseneau, D.G. Fleming, M. Senba, I.D. Reid and D.M. Garner, *Can J. Chem.*, 1988, **66**, 2018.

[42] M. Senba, D.G. Fleming, D.J. Arseneau, D.M. Garner and I.D. Reid., *Phys. Rev. A*, 1989, **39**, 3871.

[43] R.J. Duchovic, A.F. Wagner, R.E. Turner, D.M. Garner and D.G. Fleming, *J. Chem. Phys.*, 1991, **94**, 2794.

[44] Y. Morozumi, K. Nishiyama and K. Nagamine, *Phys. Letts. A*, 1986, **118**, 93.

[45] T. Sugai, T. Kondow, A. Matsushita, K. Nishiyama and K. Nagamine, *Chem. Phys. Lett.*, 1992, **188**, 100.

[46] T. Sugai, M. Sakamoto, A. Matsushita, K. Nishiyama, K. Nagamine and T. Kondow, *J. Chem. Phys. Lett.*, 1994, **101**, 2091.

[47] S.P. Cottrell, C.A. Scott and B. Hitti, *Hyp. Int.*, 1997, **106**, 251.

[48] S.P. Cottrell, C. Johnson, S.F.J. Cox and C.A. Scott, *Physica B*, 2003, **326**, 243.

[49] S.R. Kreitzmann, *Hyp. Int.*, 1990, **65**, 1055.

[50] P.W. Percival, B. Addison-Jones, J.-C. Brodovitch and S. Sun-Mack, *Appl. Magn. Reson.*, 1996, **11**, 315.

[51] J.J. Pan, D.J. Arseneau, M. Senba, D.G Fleming, U. Himmer and Y. Suzuki, *PCCP*, 2000, **2**, 621.

[52] K. Ghandi, D.J. Arseneau, M.D. Bridges and D.G. Fleming, J. Phys. Chem. A, 2004, **118**, 11613.

[53] J.I. Steinfeld, J.S. Fransisco and W.L. Hase, *"Chemical Kinetics and Dynamics"*, Prentice Hall, NY, 1998.

[54] D.G. Truhlar and B.C. Garrett, in "*Ann. Revs. Phys. Chem.*", Vol 35, pg. 159, 1984, B.S. Rabinovitch, J.M. Schurr and H.L. Strauss, eds; Ann. Rev. Inc., Palo Alto, CA.